

Supporting Information

Engineering polydimethylsiloxane with two-dimensional graphene oxide for extremely durable superhydrophobic fabric coating

Hong Yan, Hui Zhou, Qun Ye, Xiaobai Wang, Ching Mui Cho, Angeline Yan Xuan Tan and Jianwei Xu*

S1. Additional Experimental Data:

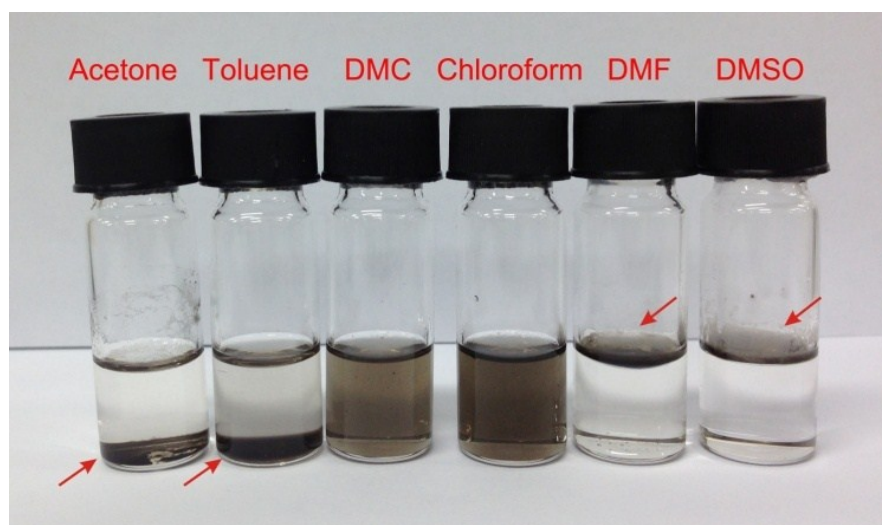


Figure S1. The photograph of PDMS/PMHS@RGO 3 in various solvents.

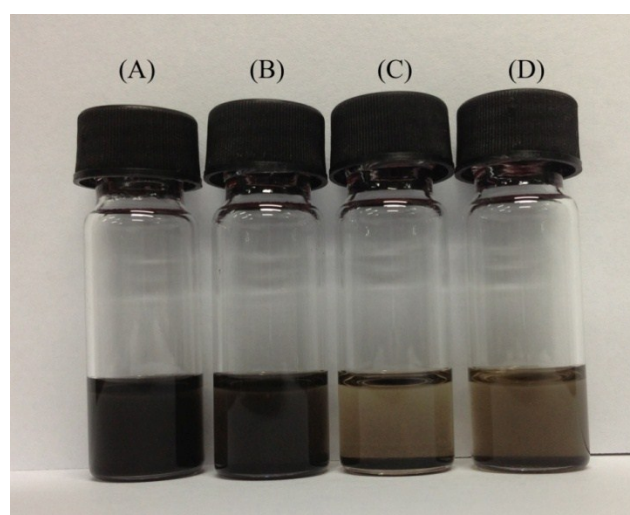


Figure S2. The photograph of Si-H terminate PDMS *m.w.* 600 – 800 (A and C) and *m.w.* 4500 – 5000 (B and D) decorated RGO and GO in toluene. (Note: (A) sample 6; (B) sample 7; (C) and (D) is the samples of corresponding Si-H terminate PDMS modified GO for comparison.

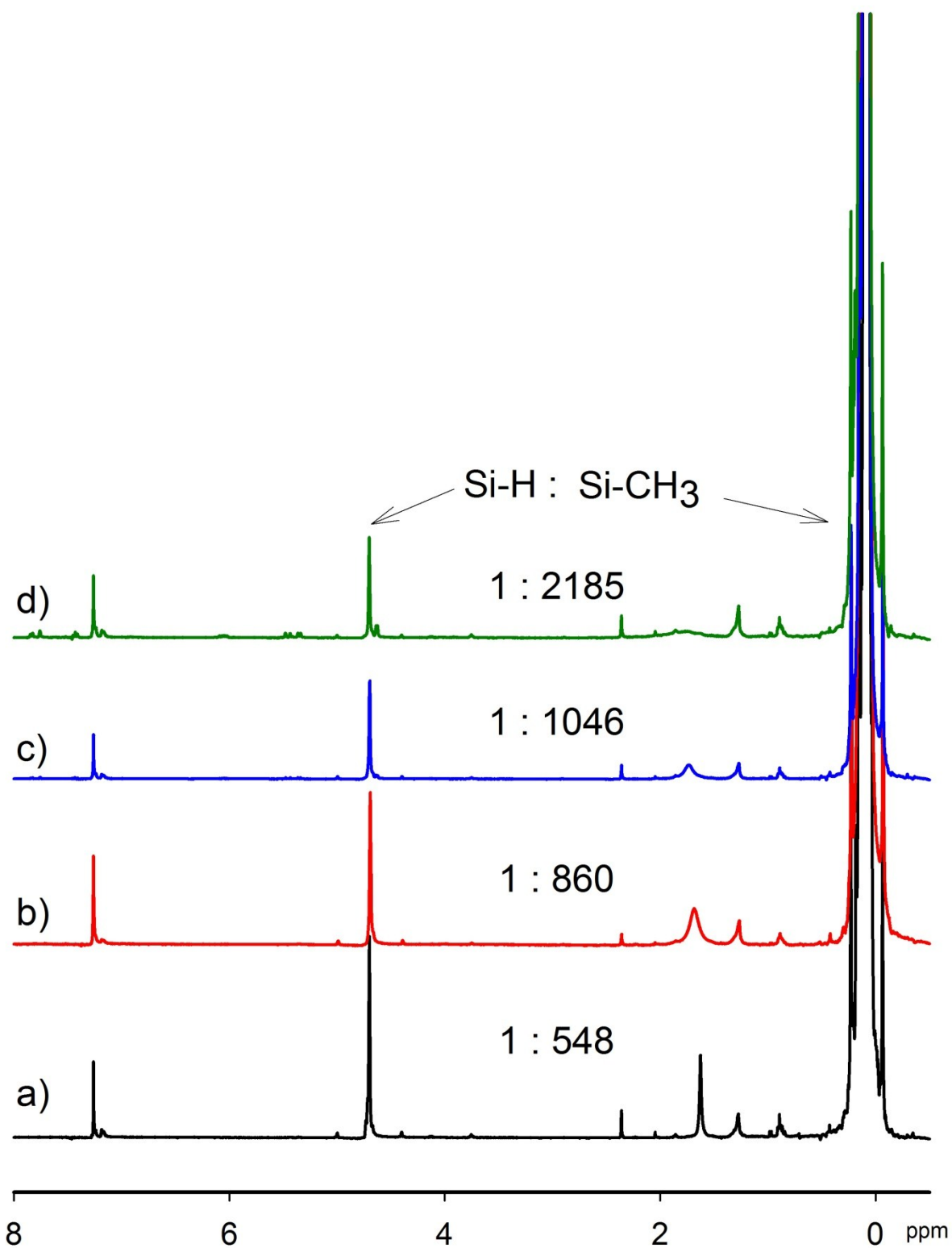


Figure S3. ^1H NMR spectra of a) PDMS/PMHS; b) PDMS/PMHS@RGO 1; c) PDMS/PMHS@RGO 2; d) PDMS/PMHS@RGO 3.

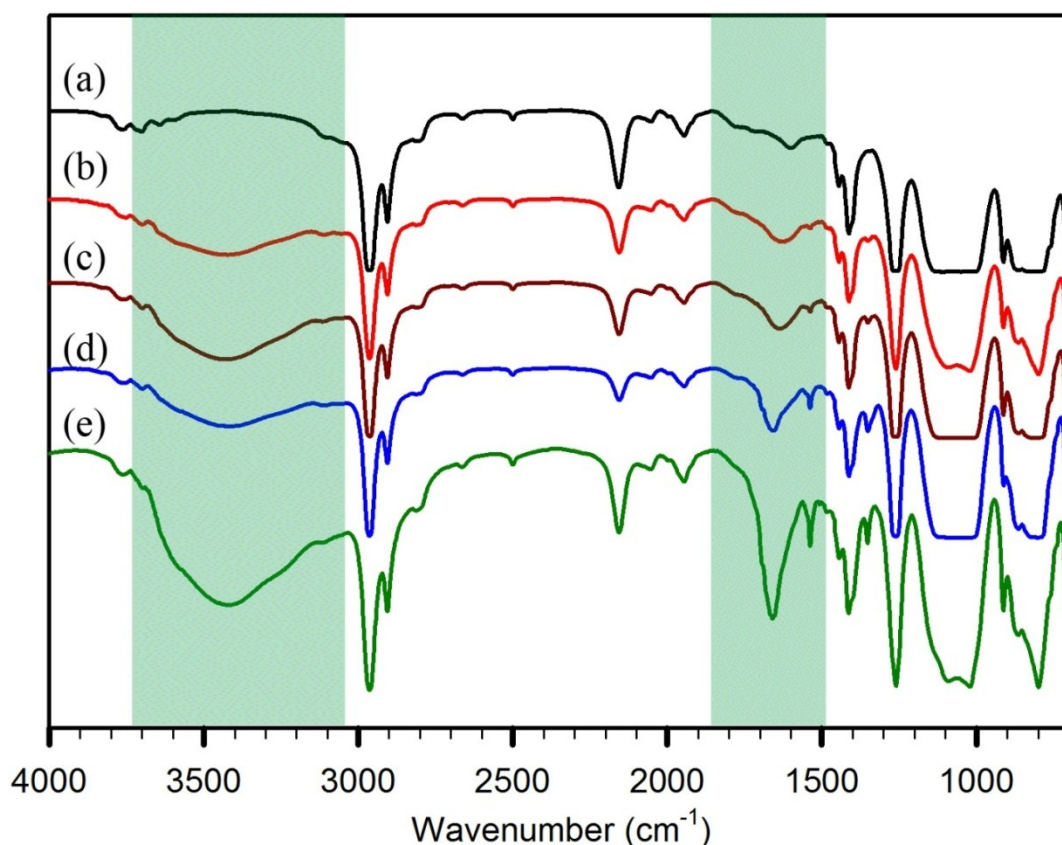


Figure S4. FTIR spectra of (a) PDMS/PMHS (*m.w.* 13 000), (b) PDMS/PMHS@RGO 1, (c) PDMS/PMHS@RGO 2, (d) PDMS/PMHS@RGO 3, (e) PDMS/PMHS@RGO 4.

Figure S4 and S5 show a set of representative FTIR spectra of pure PDMS and PDMS/PMHS@RGO composites with various compositions. All FTIR spectra of PDMS/PMHS@RGO 1 – 4 prepared by synthesis approach I show peaks around 2950, 1400 and 1260 cm⁻¹, which were assigned to Si-CH₃ groups of PDMS/PMHS. The characteristic features of their spectra showed a band of asymmetric stretching of Si-O-Si around 1100 cm⁻¹. The progressive increase in intensity of the aromatic skeletal vibration band at 1650 cm⁻¹ and hydroxyl stretching band at 3100 cm⁻¹ are evident with the increase of RGO precursor in the PDMS/PMHS matrix, indicating the effective formation of covalent bonds between RGO and PDMS/PMHS.

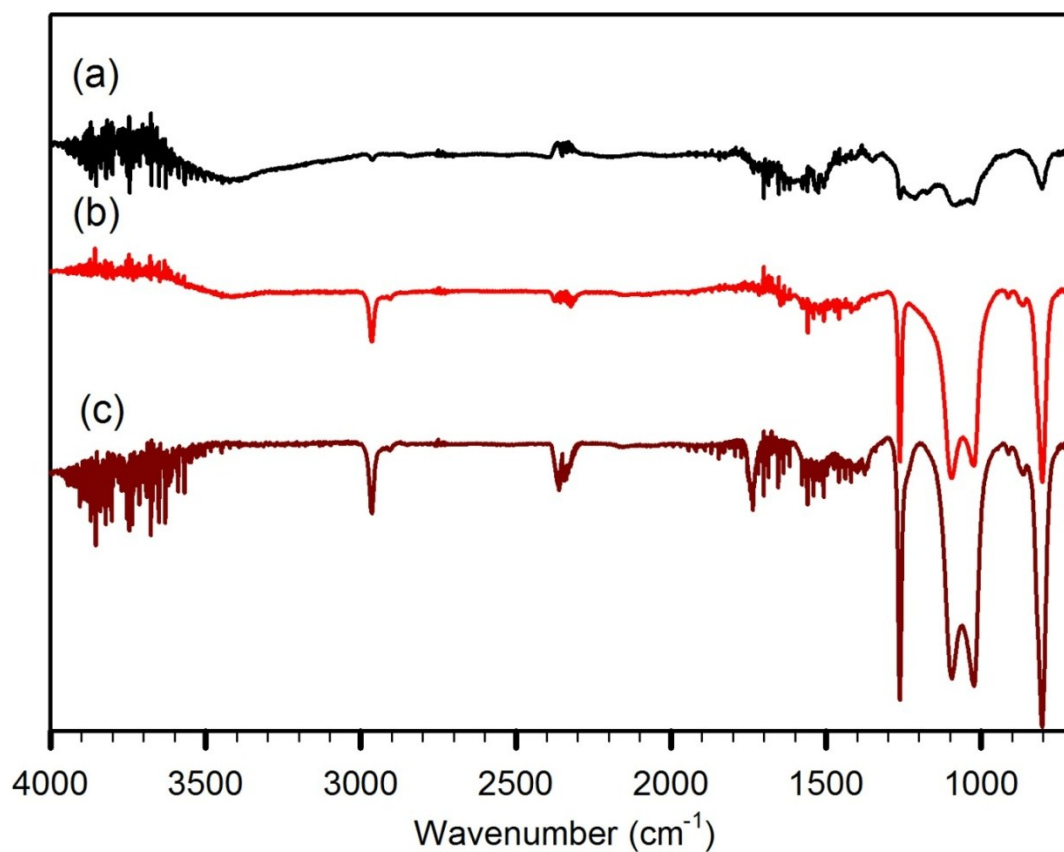


Figure S5. FTIR spectra of (a) vinyloxy benzene covered RGO, (b) PDMS@RGO 6, (c) PDMS@RGO 7.

The FTIR spectra of PDMS@RGO 6 – 7 obtained by synthesis approach II are shown in **Figure S5**. The identify peaks at 2950, 1260, 1100 and 800 cm^{-1} are observed in their respective FTIR spectrum, which corroborates the successful covalent binding between RGO and Si–H terminated PDMS.

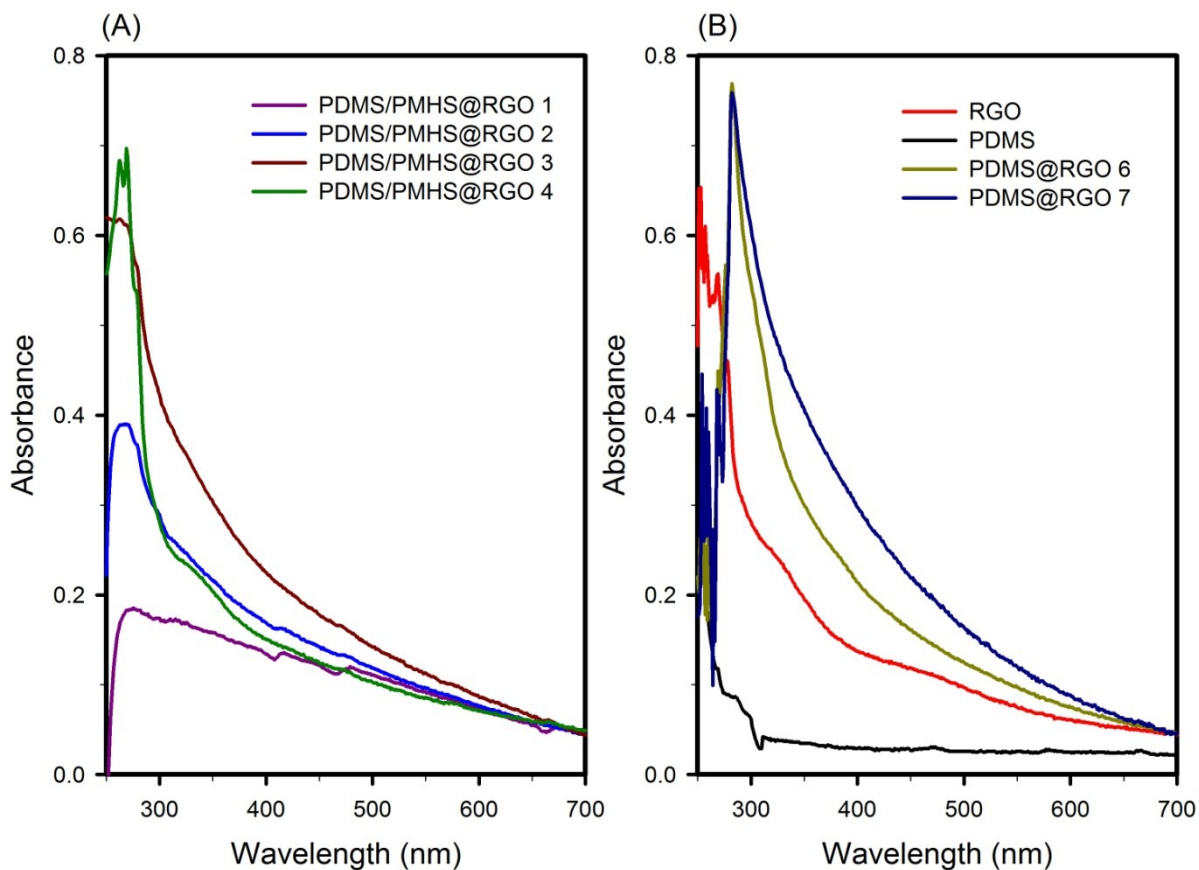


Figure S6. UV-visible spectra obtained from solutions of (A) different PDMS/PMHS@RGO 1 – 4 in chloroform and (B) vinyloxy benzene covered RGO, PDMS and PDMS@RGO 6 – 7 in toluene.

Furthermore, the UV-Vis study of PDMS/PMHS@RGO composites showed that the higher the ratio of RGO precursors, the stronger the intensity of the peaks at 260 nm (**Figure S6A**). A similar observation is found in the UV-Vis spectra of PDMS@RGO 6 and 7 (**Figure S6B**).

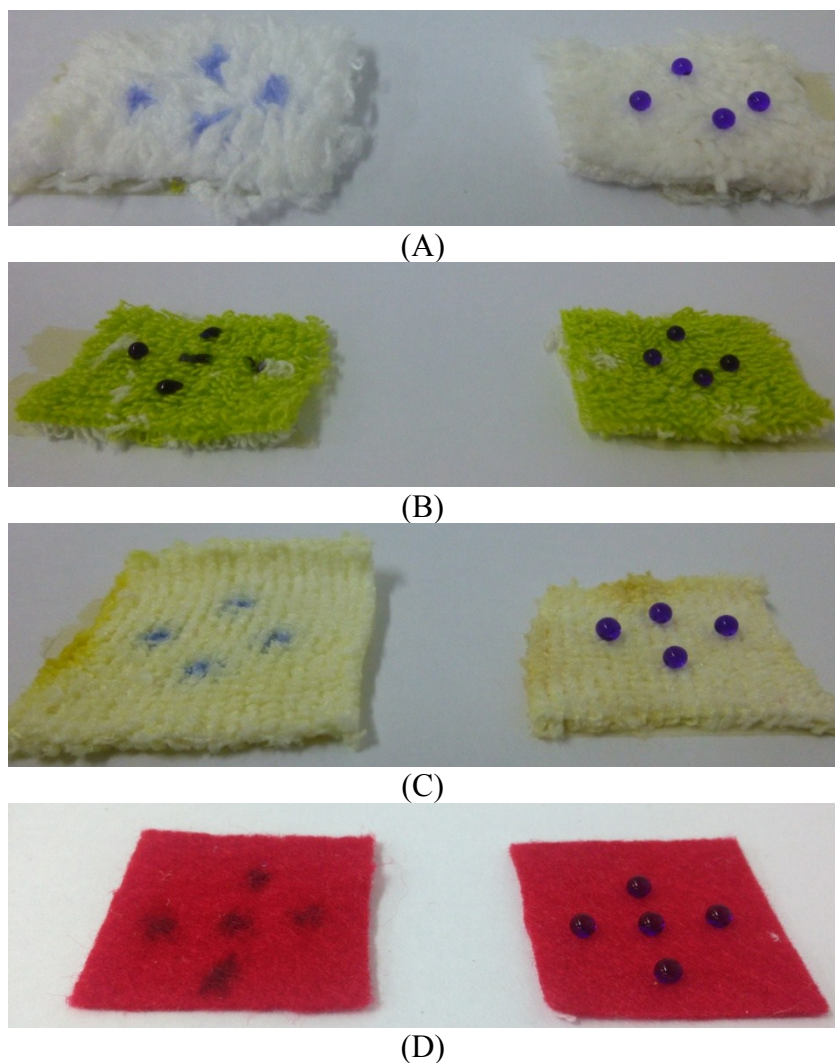


Figure S7. Wetting behavior of water on various commercial textile fabrics before and after dip coating with PDMS/PMHS@RGO 2: (A) 85 % polyester, 15 % Nylon; (B) 100 % cotton; (C) 100 % polyester; (D) 100 % polyester.

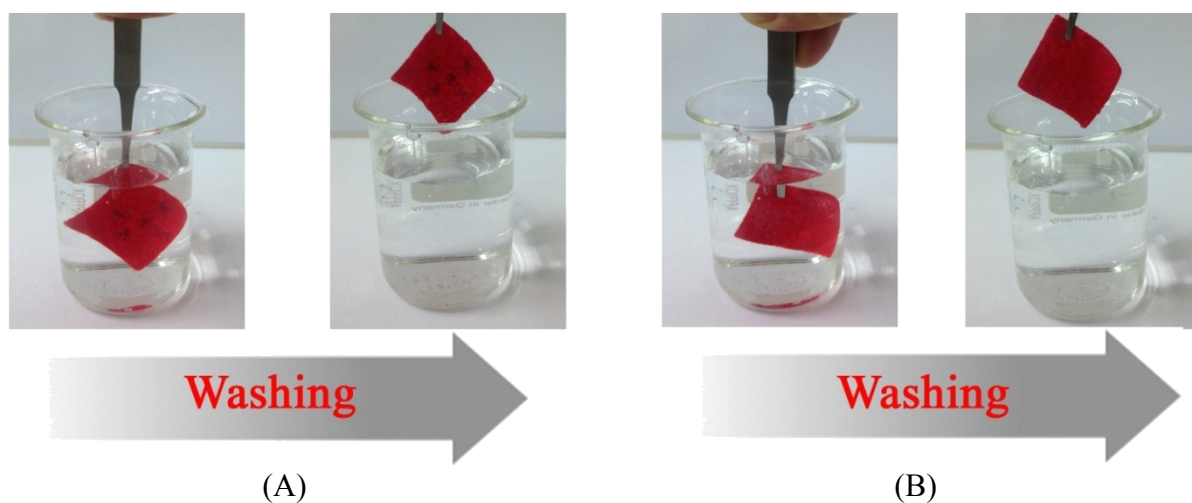


Figure S8. Stain resistant behavior of textile fabrics (A) before and (B) after dip coating with PDMS/PMHS@RGO 2.

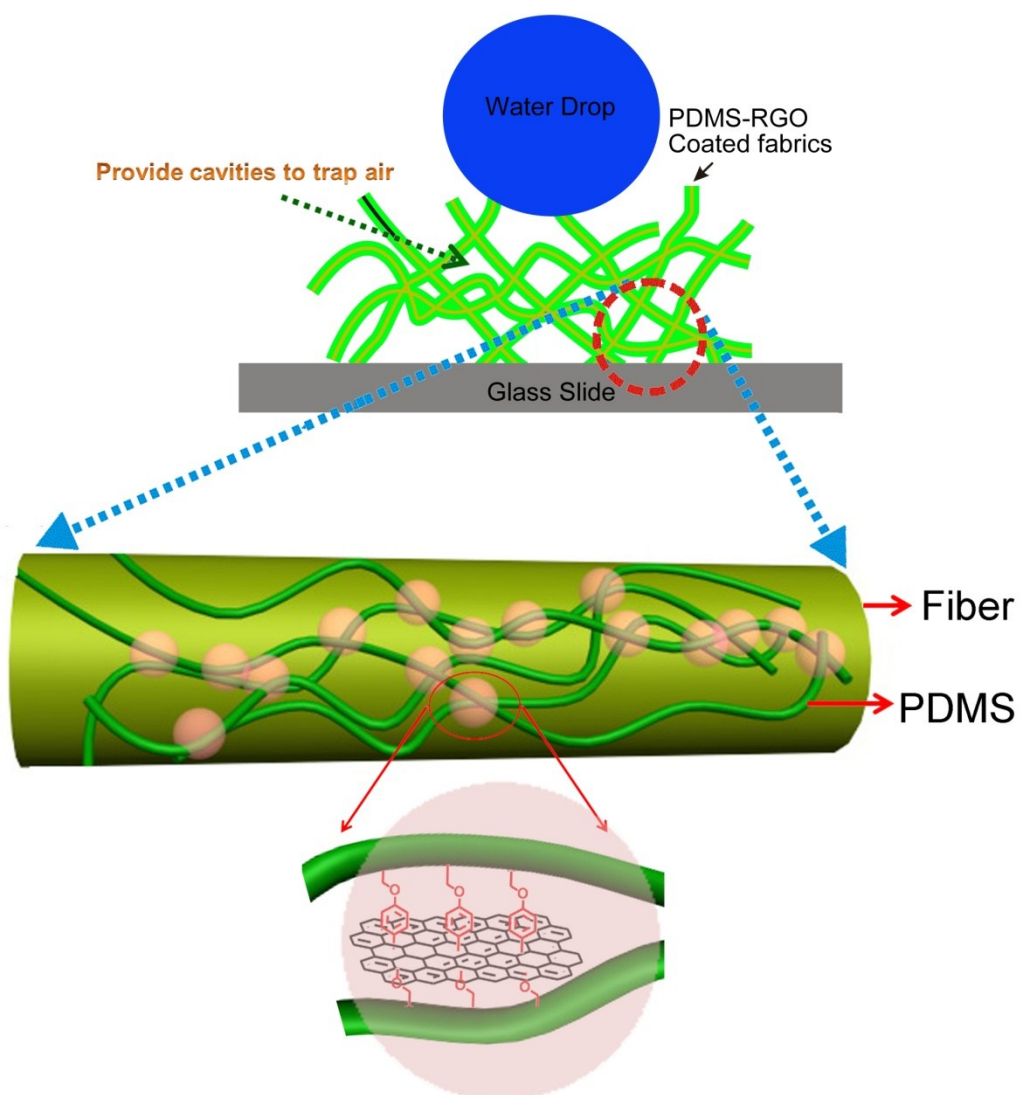


Figure S9. A graphical representation of superhydrophobic fabric-coating of PDMS/PMHS@RGO hybrid materials with hierarchical roughness; and three dimensional PDMS/PMHS–RGO hybrid materials coated on fiber.

PDMS@RGO 7



PDMS/PMHS@RGO 3



After acid etching (30 days)
(aqueous H₂SO₄ solution
pH = 1)

After base etching (30 days)
(aqueous NaOH solution
pH = 14)

**After boiling water
(2 hours)**

Figure S10. UV-visible spectra obtained from solutions of (A) different PDMS/PMHS@RGO 1 – 4 in chloroform and (B) vinyloxy benzene covered RGO, PDMS and PDMS@RGO 6 – 7 in toluene.

Table S1. Summary of static water contact angle and surface energy of different wt% of RGO (sample 1-5) in coatings on glass slide.

S. No.	Feed Ratio ^{a)} (PDMS:RGO)	Static water contact angle	Sliding angle	Advancing (θ_a) /receding (θ_r) contact angles	Contact angle hysteresis ($\theta_a - \theta_r$)	Surface energy (S.E.)		
						Polar component	Dispersive component	Total S.E.
PDMS	100 : 0	100 ± 1°	N.A. ^{b)}	85.9 / 77.1	8.8	2.84	28.58	31.42
1	3880 : 1	106 ± 1°	2°	104.2 / 102.5	1.7	0.17	23.18	23.35
2	1940 : 1	107 ± 1°	2°	101.9 / 100.7	1.2	0.08	24.65	24.73
3	776 : 1	108 ± 1°	5° <	104.2 / 101.4	2.8	0.17	24.59	24.76
4	388 : 1	117 ± 1°	5° <	106.4 / 102.3	4.1	0.23	24.73	24.96
5	194 : 1	- ^{c)}	-	-	-	-	-	-

a) Weight ratio; b) Sliding angle > 90 °; c) Data not available.

Table S2. Summary of Sliding angle of before and after washing.

S. No.	Sliding angle
0	4°
200 cycles	~12°